



日本原子力研究開発機構機関リポジトリ
Japan Atomic Energy Agency Institutional Repository

Title	Creep-fatigue evaluation method for weld joints of Mod.9Cr-1Mo steel, 1; Proposal of the evaluation method based on finite element analysis and uniaxial testing
Author(s)	Ando Masanori, Takaya Shigeru
Citation	Nuclear Engineering and Design, 323, p.463-473 (2017)
Text Version	Author Accepted Manuscript
URL	https://jopss.jaea.go.jp/search/servlet/search?5057385
DOI	https://doi.org/10.1016/j.nucengdes.2016.09.035
Right	© 2017. This manuscript version is made available under the CC-BY-NC-ND 4.0 license http://creativecommons.org/licenses/by-nc-nd/4.0/

Title

Creep-fatigue evaluation method for weld joints of Mod.9Cr-1Mo steel

Part I: Proposal of the evaluation method based on finite element analysis and uniaxial testing

Authors

Masanori Ando

Japan Atomic Energy Agency, Oarai-cho, Higashi-ibaraki, Ibaraki, 311-1393, Japan

ando.masanori@jaea.go.jp

TEL; 8129-267-4141, FAX;8129-266-3675

Shigeru Takaya

Japan Atomic Energy Agency, Oarai-cho, Higashi-ibaraki, Ibaraki, 311-1393, Japan

takaya.shigeru@jaea.go.jp

Abstract

In the present study, a method for creep-fatigue life evaluation of Mod.9Cr-1Mo steel weld joint was proposed based on finite element analysis (FEA). Since the point of the creep-fatigue life evaluation in the weld joint is a consideration of the metallurgical discontinuities, FEA was performed using a model with three material properties, a base metal (BM), weld metal (WM) and a heat-affected zone (HAZ) formed in the base metal due to the welding heat input, to consider the mutual relationships among them. The material properties of these three materials were collected and utilized in FEA for considering such metallurgical discontinuities. The creep-fatigue life estimated using the proposed evaluation method based on the FEA results were compared with available creep-fatigue test data, and the proposed method was found to predict the number of cycles to failure within a factor of 3. Moreover, the elastic follow-up factors due to metallurgical discontinuities were calculated using the FEA results for a uniaxial creep-fatigue test. The values of the elastic follow-up factors for both plastic deformation and creep relaxation were less than those defined in the Japanese elevated temperature design code. These considerations will contribute to the codification of evaluation rules for creep-fatigue damage in Mod.9Cr-1Mo steel weld joints.

Keywords

Heat-resistant steel, Fatigue, Creep-fatigue interaction, Weld joint, Elevated temperature

1. Introduction

Mod.9Cr-1Mo steel is a candidate material for the primary and secondary heat transport system components of the Japan sodium-cooled fast reactor (JSFR) [1]. In the JSFR, a shorter piping layout and rational component design have been planned. To enhance both safety and economic competitiveness, the Japan Atomic Energy Agency has proposed an attractive plant concept and extended much effort to demonstrate the applicability of innovative technologies to the plant. One of the most practical methods to enhance the economic competitiveness is to reduce the construction costs by decreasing the total quantity of required structural materials. To meet these requirements, high-Cr ferritic steel has attractive characteristics as the main structural material for sodium-cooled fast reactor (SFRs) because it has both excellent thermal properties and high-temperature strength.

To accommodate the application of this new material, the Japan Society of Mechanical Engineers (JSME) updated the design and construction codes for fast reactor (FRs) in 2012 [2]. The main topic in the 2012 edition of the JSME FRs code is the registration of two new materials: 316FR and Mod.9Cr-1Mo steel. In addition to standardizing the allowable strength values and material properties for the registration, the evaluation procedures for creep-fatigue damage and other rules were defined. Moreover, the margins for the Mod.9Cr-1Mo steel with respect to the rules were assessed to confirm that the magnitudes of the margins were appropriate for the new materials [3].

The JSME FRs code originated from design guidelines applied to the construction of the Japanese prototype fast reactor “Monju” [4-5]. These guidelines did not include a method for evaluating the weld joints because all weld joints in Monju were manufactured far from areas where primary and secondary stresses were expected to be significant. Consequently, the JSME FRs code also does not include a method for evaluating the weld joints. However, the shorter piping layout and optimized component design of the JSFR allow significant secondary stress generation under certain events at the weld joints. Therefore the development and codification of the creep-fatigue evaluation method for structural materials of the JSFR, 316FR and Mod.9Cr-1Mo steel, are required. To contribute this requirement, the creep-fatigue evaluation method for Mod.9Cr-1Mo steel welding joint was investigated in this study.

To adopt Mod.9Cr-1Mo steel, the individual failure mechanism (Type IV cracking) at the weld joints [6-8] should be considered in piping and component design. Since the evaluation procedure of primary stress limit for the weld joint of Mod.9Cr-1Mo steel is one of the important subjects for the JSFR design, the creep rupture curve of weld joints made of Mod.9Cr-1Mo steel was proposed based on the available creep rupture data and the stress range partitioning method for the evaluation of creep rupture strength [9-10]. In addition to this creep rupture curve for Mod.9Cr-1Mo steel weld joints, a provisional weld joint strength reduction factor (WJSRF) for

Mod.9Cr-1Mo steel has also been proposed to develop the rules that limit primary stress in the JSME FRs code.

Many studies have been carried out on Type IV cracking, the failure mode that originates in the heat-affected zone (HAZ), in the creep testing of weld joints [6-8]. On the other hand, with respect to failure mechanism of SFRs components, the most important failure mode to be prevented in the design is creep-fatigue. However, the studies for the evaluation of the creep-fatigue life of the weld joints of Mod.9Cr-1Mo steel are limited[11]. Since a failure mode that originated in the HAZ was also recognized through creep-fatigue testing and the available data research, we have investigated the evaluation method of creep-fatigue life for the weld joints of Mod.9Cr-1Mo steel considering the HAZ. To develop such an evaluation method, the creep-fatigue life for the weld joints of Mod.9Cr-1Mo steel was estimated using finite element analysis (FEA), and the results were compared with the available data.

Asayama et al. proposed a creep-fatigue evaluation method for the weld joints of Mod.9Cr-1Mo steel based on the FEA of a model consisting of three materials with different properties: the weld metal (WM), the base metal (BM), and the HAZ [11]. This evaluation method considers the effect of cyclic softening and accurately predicts the test results. In this method, each material region was assumed to gradually soften to half that of the number of cycles to failure, $1/2 N_f$, and creep and fatigue damages accumulate from cycle to cycle. However, the number of cycles to failure, N_f , must be known to define the number of softening cycles in this method. Thus, it is difficult to apply this method as the basis of a design rule.

In the present study, we propose a method for creep-fatigue evaluation in the weld joints of Mod.9Cr-1Mo steel for the development of design rules. A method for creep-fatigue life evaluation was proposed on the basis of the results of FEA performed using a model with three material properties that considers metallurgical discontinuities. The results estimated using the proposed evaluation method were compared with available creep-fatigue test data.

To develop a simplified method for the creep-fatigue evaluation of the weld joints, the elastic follow-up factors due to metallurgical discontinuities were calculated using the FEA results. The values of the elastic follow-up factors for both plastic deformation and creep relaxation were then compared with the values provided in the JSME FRs code, although these values are defined for structural discontinuities in the components. Using this approach, the primary concept for design rules intended to prevent creep-fatigue failure in Mod.9Cr-1Mo steel weld joints is discussed.

2. Proposed method for creep-fatigue evaluation using inelastic FEA with three material properties

The general outline of the proposed method based on FEA performed using the three materials (BM, HAZ and WM) with different properties is shown in Fig.1. In this procedure, the

creep-fatigue life is estimated individually in the BM, HAZ, and WM, and the minimum value of failure life is assumed to be the failure life of the weld joint. In the proposal procedure, performing the FEA with the entire the creep-fatigue specimen considering the test condition is needed. Next, the creep-fatigue life in the BM, HAZ, and WM is estimated using stress-strain behavior at certain points in each region. In the estimations of fatigue and creep damage, the fatigue life and creep rupture curves for the BM, HAZ and WM are applied.

To demonstrate the proposed procedure, two key items need to be developed. First, a simulation technique that allows the strain amplitude between the gauge grips (gauge length) to remain constant during the holding period of the creep-fatigue test (Fig.1). Because the creep-fatigue test is performed by controlling the strain, the strain amplitude between the gauge grips is held constant during the holding period. Since there are both metallurgical and structural discontinuities at the loading area, stress-strain redistribution occur due to creep behavior during the holding period. Therefore, when the boundary condition is defined as the constant deformation holding with the FEA model of the whole loading area, the strain amplitude between the gauge grips will change due to creep deformation during the holding period. To avoid this difference between test controlling and FEA, a technique that allows the adjustment of the boundary condition at the loading area for each historical step in a manner similar to that used in the test is required. To solve this issue, a strain feedback program was developed that automatically checks the output of strain calculated by the FEA for each step and constructs the input data of which strain amplitude remain almost constant for the next step. This strain feedback program enables the practical simulation of the strain controlling creep-fatigue test.

The second item is the development of the material properties of the BM, HAZ and WM to be assigned in the FEA. Therefore, a simulated HAZ (S-HAZ) was fabricated, and the uniaxial testing of the S-HAZ was performed to determine the material properties of the HAZ region. In addition to the S-HAZ testing, the material test results and previously reported test data were analyzed to collect the material properties. Based on these results, FEA using a model with the three different material properties was performed, and the calculated results were compared with the available test data. While only three material properties were used in the present study because of the difficulty in collecting material property data, this proposed evaluation procedure can be extended to analyses using larger numbers of materials [12].

For all evaluations, the creep-fatigue damage was estimated using the linear accumulative damage rule, and the accumulative fatigue damage (D_f) and accumulative creep damage (D_c) were evaluated individually. As a failure criterion under the superposition of creep and fatigue damage, the bilinear connecting criterion $(D_f, D_c) = (1, 0), (0.3, 0.3),$ and $(0, 1)$ proposed by Campbell was adopted for all evaluations, because the applicability of this bilinear criterion was

confirmed in the structural test of Mod.9Cr-1Mo steel with inelastic FEA using one half of the cyclic stress–strain curve [13].

3. Collection of the material property data

3.1 Material properties for FEA

For the creep-fatigue life evaluation of the weld joint using FEA, property data for the materials comprising the weld joint were required. A weld joint is roughly composed of the BM, HAZ and WM. For simplification, in the present study, the properties of these three materials were focused. The material properties for the BM were obtained from the JSME FRs code [2] and its supporting documentation [3]. The material properties of the HAZ were experimentally obtained using uniaxial tests. However, because obtaining a test specimen composed only of the HAZ is impossible, an S-HAZ sample was prepared for uniaxial tests by heat treatment. The fatigue properties of the WM were obtained from the literature [14], and the creep properties of the WM were obtained from other available data [15].

3.2 Material properties of the S-HAZ

The material properties of the HAZ were obtained by testing an S-HAZ specimen. The S-HAZ was produced by an additional heat treatment of the raw material. To define the additional heat treatment conditions for obtaining an appropriate S-HAZ specimen, the microscopic observation of a section of a Mod.9Cr-1Mo steel plate weld joint and the Vickers hardness test of the same weld joint were performed. Based on the results, the condition for the additional heat treatment of the raw metal and the width of the HAZ in the FEA model were estimated. The weld joint for these observations and Vickers hardness test was produced via tungsten inert gas welding using a 25-mm thick plate. The chemical compositions of the BM and WM are summarized along with the heat treatment conditions in Table 1. The results of the Vickers hardness test using a 500-g weight are shown in Fig.2. The test was performed along three lines (1/4, 1/2, and 3/4 sections). The region near the base material with the lowest hardness was defined as the HAZ to be simulated. The hardness of this region was approximately $HV = 210$, and the width was estimated to be approximately 2 mm. To produce the S-HAZ, we attempted to fabricate a material with hardness and grain size similar to those of the HAZ region in the original weld. However, duplicating both values exactly in the S-HAZ specimen was difficult. Therefore, the hardness value in the S-HAZ was adjusted to correspond to that of the HAZ in the weld joint ($HV = 210$, Fig.2) because this value is numerically clearer than the grain size. Using optical microscopy, the grain size number (ASTM E 112) in the BM and HAZ of the original weld joint were estimated to be 8.0 and 10 to 12, respectively.

Based on the experimental survey of a heat treatment, an S-HAZ with average $HV = 213$ was

produced by normalizing at 890 °C followed by water quenching, and then holding at 740 °C for 8.4 h in a furnace. Using optical microscopy, the grain size number of this S-HAZ sample was estimated to be 9.5.

The fatigue test results for the S-HAZ specimen are shown in Fig.3. The number of cycles to failure, N_f , for the S-HAZ was slightly less than that for the BM; however, the cyclic stress–strain curve for the S-HAZ shown in Fig.4 was nearly the same as that for the BM (three plots are shown to overlap in the strain range of 0.5% in Fig.4). Because the obtained data points were limited and considering the variations in N_f during the fatigue test, the cyclic properties of the HAZ were assumed to be the same as those of the BM.

The creep test results for the S-HAZ are shown in Fig.5. The rupture times for the S-HAZ were also nearly the same as those for the BM at 550 °C. On the other hand, the rupture times for the S-HAZ were shorter than those of the BM at 600 °C. In addition, the minimum creep strain rates for the S-HAZ sample were slightly and significantly faster at 550 °C and 600 °C, respectively, as shown in Fig.6. These tests results of the creep rupture time (Fig.5) and the minimum creep strain rate (Fig.6) at 600 °C were supposed to be comparable to the equation for the BM with time factor, (α_R), of 10 provided by the JSME FRs code. This time factor reduces the creep rupture time of the BM by a factor of 10. This application of $\alpha_R = 10$ is also accelerated the creep relaxation rate because the creep strain equation in the JSME FRs code uses the creep rupture equation that incorporates the time factor. Taking into account that the test at 600 °C was performed as an accelerated-temperature test, these properties are supposed to appear in the long term creep testing at 550 °C. Therefore, considering the creep test results at 600 °C, the creep properties for the HAZ were assumed to be those in the JSME FRs code with an applied time factor of 10.

3.3 Material properties of the weld metal

The fatigue properties of the WM have been reported in a previous study [14]. The fatigue life in the WM was slightly shorter than that in the BM and corresponded to the nominal curve in the JSME FRs code with the strain range increased by a factor of 1.1. In addition, the cyclic stress–strain curve for the WM was larger than that in the BM and corresponded to the curve in the JSME FRs code with the offset yield strength increased by a factor of 1.1. Therefore, these assumptions were adopted in the present study.

The creep properties in the WM were obtained from the available data shown in Fig.7 and Fig.8 [15]. The creep strength and minimum creep strain rate were found to be comparable to the values in the JSME FRs code.

4. Evaluation of the test results

4.1 Assigned material properties for the FEA

The material properties used for the FEA are summarized in Table 2. The material properties in the JSME FRs code (Tables A1 to A4) were modified on the basis of the values in Table 2. To account for the cyclic softening characteristics of Mod.9Cr-1Mo steel, one half of the cyclic stress–strain curve was applied for the FEA. Notably, Mod.9Cr-1Mo steel is gradually softened by cyclic loading; thus, the application of a complex kinematic model to simulate this behavior may be more reasonable. Nevertheless, the primary objective of this study was to develop a method for evaluating the creep-fatigue life of the weld joints in order to develop a design rule, not to simulate the changes in material responses. Therefore, a stable stress–strain response represented by one half of the cyclic stress–strain curve was assumed to be adequate for this study. For simplicity, we simulated monotonic tension and holding condition in FEA to estimate the stress-strain redistribution during plastic and creep deformation, not perform the cyclic change analysis. Therefore, a multilinear stress-strain relation was used with isotropic hardening rule. This was one of the reasons to use one half of the cyclic stress–strain curve.

Both elastic and inelastic FEAs were performed using the FINAS code [16]. Here, inelastic FEA means elastic-plastic-creep FEA, and the eight-node quadri-lateral axisymmetric elements QAX8 of the FINAS code were utilized for all calculations in this study.

4.2 FEA model and analysis of the fatigue test

To simulate the strain distribution in a specimen during the fatigue test, a nominal test specimen was modeled for the FEA (Fig.9). The welding line was located at the center of the gauge length in this model, and the volume ratio between the gauge grips (gauge length) was the same in the WM and BM containing the HAZ. Because one half of the cyclic stress–strain response was assumed to be the same in the BM and HAZ, the analytical model for the fatigue test is based on two types of material properties: those for the BM and WM. The end of the model was tensioned until the strain range in the gauge length approached the test conditions. The obtained stress and strain distributions along the specimen surface are shown in Fig.10. The maximum equivalent strain was generated at the BM closer to the center side and was located approximately 3.5 mm from the center of the specimen. In addition, the difference in the maximum equivalent strain for the WM and BM increased as the strain range increased. The fatigue lives of the BM and WM were evaluated using the maximum strain range in each region. The integral point generating the maximum strain range in the BM was used to estimate the fatigue life of the BM. On the other hand, to estimate the fatigue life for the WM, the strain range for the neighboring integral point at the center of the specimen was used. The strain range for the WM was then multiplied by 1.1 and applied as the nominal fatigue curve for the BM in the JSME FRs code. The estimated results are shown in Fig.11 along with the available test data [15]. As shown in this figure, the fatigue life was estimated for various strain ranges, and these results are connected with a line. Therefore,

there are a total of three lines. The first is the nominal fatigue curve described in the JSME FRs code. The second and third lines are the BM and WM failure curves for the weld joint estimated by inelastic FEA. Figure 11 clearly shows that the BM failure curve indicates a shorter failure life. This suggests that the fatigue life of the weld joints depended on the strain range generated at the BM. Using the FEA, the fatigue failure was confirmed to generally occur in the BM or at the BM–WM boundary in low-cycle fatigue, and this tendency corresponded to the test results. In addition, the FEA results indicated that there is a possibility for a change in the main failure location from the BM to the WM in high-cycle fatigue tests with more than 100,000 cycles. This prediction seems to explain one test result of the WM failure plotted in the strain range of 0.4% - 31,875 cycles.

4.3 FEA model and calculated results of creep-fatigue test

To simulate the strain distribution in the specimen during the creep-fatigue test, a nominal test specimen was modeled for the FEA that also included the three types of materials (WM, BM, and HAZ) (Fig.12). Because the fatigue test and creep-fatigue test were performed in different testing machines, the specimen configuration in Fig.12 differs from that in Fig.9. The welding line was located at the center of the gauge length in the specimen model of this creep-fatigue test, and the volume ratio between gauge grips (gauges length) was different from that of the fatigue specimen shown in Fig.9. To avoid the effect of boundary conditions on the stress-strain redistribution during creep relaxation, the entire specimen was modeled when simulating the creep-fatigue test. As shown in Fig.12, the entire region of the WM was located within the gauge length. FEA was performed such that the experimental conditions were simulated. Because the creep-fatigue test was performed by controlling the strain amplitude, the total strain amplitude in the gauge length generated by the tension loading of the model end was monitored for each historical step in the FEA. The displacement of the model end was controlled for each step such that the total strain amplitude in the gauge length corresponded to the experimental settled strain amplitude during holding. Therefore, before holding, the model end was tensioned until the setup strain amplitude was reached, and the displacement boundary condition was then adjusted according to the creep behavior. This FEA technique was applied because the strain distribution in the specimen changed during holding due to creep relaxation. Without this strain feedback technique, strain amplitude within gauge length is changed by stress-strain redistribution due to creep behavior during the holding.

The calculated results for the equivalent stress and strain along the specimen surface for a simulated test with strain amplitude equal to 0.25% (simulating a 0.5 % strain range test) are shown in Fig.13. When holding was initiated, relatively larger stress amplitude was generated at the boundary between the WM and HAZ (Fig.13(a)). This relatively larger stress was generated

because of the difference in the yield strength between the WM and HAZ. On the other hand, the maximum strain amplitude was generated in the BM on the center side (Fig.13(b)) when holding was initiated.

With stress-strain redistribution occurring because of creep behavior during holding, the strain was concentrated at the boundary between the HAZ and the other two materials, and the maximum strain amplitude was generated at the boundary between the HAZ and BM on the center side. On the other hand, the strain amplitude of the WM decreased during holding. This result suggests that the stress-strain redistribution was caused by elastic follow-up phenomena. In other words, as well as structural discontinuities, the metallurgical discontinuities caused stress-strain redistribution. In fact, the smooth specimen comprising a weld joint that was used for the uniaxial test was structurally continuous, but it had metallurgical discontinuities. Therefore, these results revealed that the results of the uniaxial test for the weld joints should not be evaluated in the same manner as the results of ordinary uniaxial tests for base materials.

4.4 Estimated results of the creep-fatigue life of a weld joint using the proposed procedure

The creep-fatigue test of a controlled strain range equal to 0.5% and 1.0% with a series of holding times was simulated using the proposed procedure (Fig.1). The results along with the available experimental data are shown in Fig.14 [15][17]. The estimated results indicated that the value of N_f was smallest for the HAZ at all holding times. Notably, the superposition of the strain concentration due to the larger yield strength of the WM in the plastic region and the larger creep strain rate in the HAZ during relaxation resulted in a much smaller N_f value for the HAZ. These results are in good agreement with the experimental results; nearly all specimens failed at the interface between the BM and WM or HAZ [15]. The experimental data were plotted around the predicted failure life of the BM and WM, and the predicted failure life of HAZ was lower compared to all the experimental data in both Fig14(a) and Fig14(b). When the minimum value of N_f is assumed as the creep-fatigue life for the weld joints, all experimentally determined N_f values were larger. In addition, the predicted N_f values for the WM and BM were comparable. These results suggest that the creep-fatigue life of Mod.9Cr-1Mo steel weld joints depends on the interactions between the HAZ and other materials because of their different properties.

A comparison of the N_f values obtained experimentally and those predicted using the proposed procedure is shown in Fig.15. Importantly, the N_f values were estimated using the proposed FEA analysis method were within a factor of 3. All experimental data underestimated the N_f values according to the proposed procedure. These results indicate that the proposed procedure provides conservative estimation of creep-fatigue life.

The overestimation of failure cycles in Fig.15 is attributed to the fact that the estimated creep-fatigue test data were limited at 550 °C and the most of the data were obtained by the test

with 1.0 h or less holding, while there were each one data obtained with 3.0 h and 10.0 h holding. In the practical design, long term elevated temperature holding will be supposed, and the creep damage is calculated at the smaller stress amplitude during the relaxation on the basis of the Robinson's damage accumulation rule. Therefore, considering the creep test results at 600°C, the creep properties for the HAZ were assumed to be those in the JSME FR code with an applied time factor of 10. However, the creep damage in the creep-fatigue test applied in the evaluation was limited, because these tests were performed in short time holding and not temperature-accelerated. To confirm the validity of the proposed evaluation method, a long term holding test at 550 °C and the test result at 600 °C may be required.

5. Stress-strain redistribution analysis

5.1 Stress-strain redistribution due to plastic deformation

The proposed procedure for the evaluation of creep fatigue in Mod.9Cr-1Mo steel weld joints using FEA based on three materials enabled the adequate estimation of N_f values. Because inelastic FEA using a model with welding lines in the components was not practical in the components design, a procedure based on elastic FEA is required. Inelastic FEA is a useful tool; however, it is not suitable for evaluating all components of a design. In the JSME FRs code, creep-fatigue damage is calculated on the basis of the results of elastic analyses using a simplified technique; namely, the inelastic behavior of the material at structural discontinuities in components is estimated from the results of the elastic analysis using the modified Neuber's law or the elastic follow-up method described in the code. The modified Neuber's law employed in the JSME FRs code is the same as that in the ASME Sec.III Div.1 Sub. NH T-1432(a) [18]. The elastic follow-up method was originally developed in Japan, and a value of $q = 3$ was defined in the code as a conservative value [4] [5]. Notably, the elastic follow-up factor q can be divided into q_p for elastic-plastic behavior and q_c for creep-relaxation behavior, although the JSME FRs code does not divide them in order to simplify the rules. For plastic behavior, either the modified Neuber's law or the elastic follow-up method can be applied. On the other hand, only the elastic follow-up method is applied to estimate the creep relaxation behavior.

Creep-fatigue specimens for uniaxial testing are smooth in configuration, but elastic follow-up is caused by the metallurgical discontinuities in the test of the weld joints. Therefore, the elastic follow-up behavior in the specimen was analyzed as part of the evaluation procedure intended to establish the design code.

The relationship between the elastic follow-up factor and the maximum equivalent stress on the surface is shown in Fig.16. The elastic follow-up factor for plastic deformation, q_p , was defined by

$$q_p = \frac{\Delta \varepsilon_p}{(\Delta \sigma_{el} - \Delta \sigma) / E} \quad (1)$$

where, $\Delta \varepsilon_p$ is the plastic strain range calculated using inelastic FEA, $\Delta \sigma_{el}$ and $\Delta \sigma$ represent the stress ranges calculated using elastic and inelastic FEA, respectively, and E is the elastic modulus. The elastic follow-up factor was calculated by comparing the results of the elastic and inelastic FEAs [19]. Namely, the stress and strain of the integral point where the maximum strain was calculated in the inelastic FEA was decided to be compared, then the elastic follow-up factor was calculated in the each stress level. The elastic follow-up factor was calculated from the equivalent stress and strain.

The calculated elastic follow-up factor, q_p , changed significantly at the initiation of plastic deformation. The maximum value of q_p was calculated to be approximately 2.1 in the HAZ, and a negative value was calculated for the WM because it was assigned a harder material property. As the stress range increased, the calculated values of q_p for the BM and HAZ decreased and approached approximately 1.4.

5.2 Stress-strain redistribution due to creep deformation

The elastic follow-up factor for creep relaxation, q_c , was also calculated by comparing the elastic and inelastic FEA results of the creep-fatigue test with a controlled strain range of 0.5%. The relationship between q_c , and holding time is shown in Fig.17. The q_c was defined by

$$q_c = \frac{\Delta(\varepsilon_p + \varepsilon_c)}{(\Delta \sigma_{el} - \Delta \sigma) / E} \quad (2)$$

where, $\Delta(\varepsilon_p + \varepsilon_c)$ is the sum of the plastic and creep strain ranges calculated using inelastic FEA. A larger value of q_c (approximately 1.4) was obtained for the HAZ.

Therefore, the values for both the elastic follow-up factors q_p and q_c , where elastic follow-up was caused by the metallurgical discontinuities in the weld joint, were less than $q = 3$ as defined in the JSME FRs code. These results imply that the simplified method for evaluating the structural discontinuities in the JSME FRs code can be applied to the evaluation of the metallurgical discontinuities in Mod.9Cr-1Mo steel weld joints. In other words, the elastic follow-up method may be applicable to the evaluation of smooth Mod.9Cr-1Mo steel weld joints.

Under operating conditions with low primary stress, the equation for estimating the total strain range, ε_t , in the strain concentration region exhibiting elastic follow-up behavior in the JSME FRs

code is as follows:

$$\varepsilon_t = K_\varepsilon \varepsilon_n, \quad (3)$$

where ε_n is the nominal strain range, and K_ε is defined by

$$K_\varepsilon = KK'_e, \quad (4)$$

where

$$Sn > 3\bar{S}_m, \text{ and} \quad (5)$$

$$K'_e = 1 + (q - 1) \left(1 - 3\bar{S}_m / S_n \right). \quad (6)$$

In the equation (5) and (6), Sn is the nominal stress range, K is the stress concentration factor, and $q = 3$. The parameter $3\bar{S}_m$ is same as definition in ASME Sec.III Div.1 Subsection NH, Nonmandatory appendices T1324. Note that the value of the strain concentration factor K_ε is defined as the larger of the value calculated using the modified Neuber's law and the elastic follow-up method in the JSME FRs code. The evaluation of equations (3) through (6) represented a procedure for estimating the strain concentration using the elastic follow-up method.

The FEA results rearranged according to the above equations are shown in Fig.18. The strain concentration factors, K_ε , for the BM, HAZ, and WM were less than the results obtained using equations (4) through (6) based on elastic FEA. The comparable K_ε values for the BM and HAZ were assumed by applying a value of $q = 1.3$ to the elastic FEA. As a result, the calculated strain ranges using the series of equations were larger than those obtained using the inelastic FEA method.

With respect to the creep damage calculations, in the JSME FRs code, the initial stress for creep relaxation in each cycle is defined by the strain range to estimate the fatigue damage; namely, the initial stress was determined from the tensile curve entered at estimated strain range, ε_t , in equation (3). The tensile curve was applied to consider the cyclic softening characteristics of Mod.9Cr-1Mo steel [3]. A comparison of the creep damages estimated for the BM, HAZ, and WM calculated using the elastic follow-up method is shown in Fig.19. In Fig.19, a degradation factor for creep damage, α_R , of 10 was also applied to calculate the creep damage in the HAZ. Larger creep damage during relaxation was estimated because of the conservative initial stress assumption in the procedure of the JSME FRs code, and it was also larger than that calculated for

the HAZ. The comparable creep damage in the HAZ can be assumed by applying a value of $q_c = 1.3$ to the elastic FEA.

These estimated results of elastic follow-up factors can be summarized as follows. The elastic follow-up factors of q_p and q_c for HAZ were estimated as about 1.4 when these estimated from the comparison of the results between the elastic and inelastic FEA. On the other hand, these were estimated about 1.3 when these calculated backward from the evaluation procedure described in the JSME FRs code.

These results indicated that the elastic follow-up method developed for estimating the strain concentration at structural discontinuities is applicable to the metallurgical discontinuities in Mod.9Cr-1Mo steel weld joints; however, the results were only validated by uniaxial tests of a specimen without structural discontinuities. Notably, the weld joints in the components and/or piping where significant stress is expected to be generated will be constructed using full penetration welding without structural discontinuities. Since the above-mentioned can be assumed in the uni-axial test specimen, the development of an evaluation procedure based on the structural tests and FEA of the components and piping with weld joints is needed. Note that the validation of the procedure with respect to long-term holding and harmonization of other rules should be confirmed for codification.

6. Conclusion

A method for the creep-fatigue evaluation of Mod.9Cr-1Mo steel weld joints was proposed based on inelastic FEA performed using three different materials. To perform the FEA, the material properties of the HAZ were obtained from uniaxial test data, and available data for the WM were collected. Inelastic FEA for the uniaxial creep-fatigue test was performed to confirm the stress and stress-strain redistribution during the test due to metallurgical discontinuities. Based on the obtained stress and strain redistribution, the creep-fatigue life was estimated using the proposed evaluation procedure. Moreover, the elastic follow-up factor was calculated to aid in the codification of the weld joint evaluation procedure. The main conclusions are summarized as follows:

- 1) The proposed method can predict the number of cycles to failure for available creep-fatigue test data within a factor of 3.
- 2) FEA performed using the material property data for the three materials (BM, HAZ, and WB) and the strain feedback technique allowed the simulation of the redistribution of stress and strain during the creep-fatigue test.
- 3) The elastic follow-up factor in the uniaxial test specimen during the creep-fatigue test was estimated to be less than 3.

Acknowledgement

This paper includes results for the “Technical development program on a commercialized FBR plant” entrusted to the Japan Atomic Energy Agency (JAEA) by the Ministry of Economy, Trade, and Industry of Japan (METI). The authors are grateful to Mr. Yasuhiko Inoue of ASEND, Ltd, for performing the FEA.

References

- [1] Aoto, K., Uto, N., Sakamoto, Y., Ito, T., Toda, M., Kotake, S., 2011. Design study and R&D progress on Japan sodium-cooled fast reactor. *J. Nucl. Sci. Technol.* 48, 463–471.
- [2] Japan Society of Mechanical Engineers: Codes for Nuclear Power Generation Facilities, Rules on Design and Construction for Nuclear Power Plants, Section II Fast Reactor Standards, 2012, JSME S NC2-2012 (in Japanese)
- [3] Ando, M., Watanabe, S., Kikuchi, K., Otani, T., Satoh, K., Tsukimori, K. and Asayama, T., 2013. Development of 2012 Edition of JSME Code for Design and Construction of Fast Reactors (6) Design margin assessment for the new materials to the rules. Proceedings of ASME 2013 Pressure Vessels and Piping Division Conference, PVP2013-97803.
- [4] Iida, K., Asada, Y., Okabayashi, K., Nagata, T., 1987a. Construction codes developed for prototype FBR Monju. *Nucl. Eng. Des.* 98, 283–288.
- [5] Iida, K., Asada, Y., Okabayashi, K., Nagata, T., 1987b. Simplified analysis and design for elevated temperature components of Monju. *Nucl. Eng. Des.* 98, 305–317.
- [6] Tabuchi, M., Takahashi, Y., 2006. Evaluation of Creep Strength Reduction Factors for Welded Joints of Modified 9Cr-1Mo Steel (P91). Proceedings of ASME 2006 Pressure Vessels and Piping Division Conference, PVP2006-ICPVT11-93350.
- [7] Watanabe, T., Tabuchi, M., Yamazaki, W., Hongo, H., Tanabe, T., 2006. Creep damage evaluation of 9Cr-1Mo-V-Nb steel welded joints showing Type IV fracture. *International Journal of Pressure Vessels and Piping*, No.83, pp.63-71
- [8] Hongo, H., Tabuchi, M., Takahashi, Y., 2009. Microstructures and Type-IV creep damage of high Cr steel welds. *Journal of solid mechanics and material engineering*, Vol.3, No.3, pp.464-474
- [9] Wakai, T., Nagae, Y., Onizawa, T., Obara, S., Xu, Y., Otani, T., Date, S., Asayama, T., 2010. Creep strength evaluation of welded joint made of modified 9Cr-1Mo steel for Japanese Sodium cooled Fast Reactor (JSFR). Proceedings of ASME 2010 Pressure Vessels and Piping Division Conference, PVP2010-26014.
- [10] Wakai, T., Onizawa, T., Kato, T., Date, S., Kikuchi, K., Satoh, K., 2013. A study for proposal of welded joint strength reduction factors of modified 9Cr-1Mo steel for japan sodium cooled fast reactor (JSFR). Proceedings of the ASME 2013 Pressure Vessels and Piping

Conference PVP2013, PVP2013-97091.

- [11] Asayama, T., Hasebe, S., Hirakawa, Y., Wada, Y., 1993. Creep-fatigue evaluation method for Mod.9Cr-1Mo weldment. Transaction of the structural mechanics in reactor technology, L05/5, pp.123-128
- [12] Murakami, E., Hashimoto, M., Kikuhara, S., 2012. Prediction of creep void growth in heat-affected zone of high chromium steel weldments considering multiaxial stress state. Proceedings of the ASME 2012 Pressure Vessels and Piping Conference PVP2012, PVP2012-78693
- [13] Ando, M., Hirose, Y., Karato, T., Watanabe, S., Inoue, O., Kawasaki, N., Enuma, Y. “Comparison and assessment of the creep-fatigue evaluation methods with notched specimens made of Mod.9Cr-1Mo steel,” Journal of Pressure Vessel Technology, Volume 136, Issue 4, p.041406_1 - 041406_10
- [14] Takaya, S. Evaluation of fatigue strength of similar and dissimilar welded joints of modified 9Cr-1Mo steel, Proceedings of the 22th international conference on nuclear engineering, ICONE22-30022
- [15] Kato, S., Furukawa, T. and Yoshida, E., 2008, Material Test Data of Mod.9Cr-1Mo Steel (1). JAEA-Data/Code 2008-030, in Japanese.
- [16] Japan Atomic energy agency and Itochu Techno-Solutions, 2008, FINAS User’s Manual Ver.19.0, (in Japanese)
- [17] Takahashi, Y. 2008, Study on Predictability of Creep-fatigue Life of High-chromium Welded Joint, Proceedings of JSME Conference on Mechanics and Materials, OS 1308, in Japanese.
- [18] ASME boiler and pressure vessel code section III, subsection NH, ASME (2012)
- [19] Kasahara, N., Nagata, T., Iwata, K., Negishi, H. Advanced creep-fatigue evaluation rule for fast breeder reactor components: generalization of elastic follow-up model. Nuclear Engineering and Design, Vol. 155, pp.499-518, 1995

Appendix

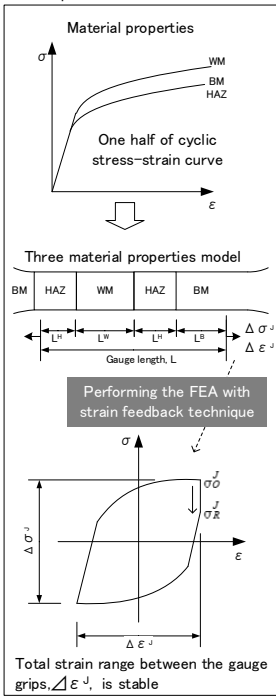
The material properties used in this study were as follows.

List of figures

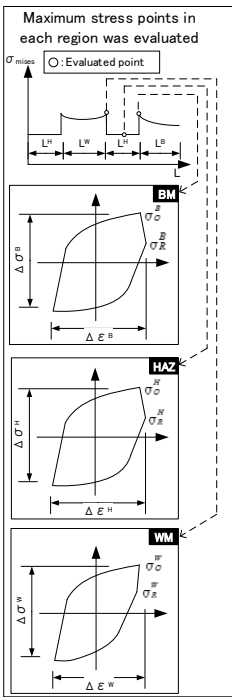
- Fig.1 Procedure for the evaluation of weld joints using FEA with three material properties
- Fig.2 Results of Vickers hardness tests for weld joints
- Fig.3 Fatigue test results for the simulated HAZ
- Fig.4 Cyclic stress–strain response for the simulated HAZ during fatigue testing
- Fig.5 Creep test results for the simulated HAZ
- Fig.6 Minimum creep strain rate of the simulated HAZ during creep testing
- Fig.7 Creep test results for the WM
- Fig.8 Minimum creep strain rate for the WM during creep testing
- Fig.9 FEA model for fatigue testing
- Fig.10 Equivalent strain redistribution in a fatigue specimen
- Fig.11 Comparison of fatigue life curves in weld joints estimated from the FEA
- Fig.12 FEA model for creep-fatigue testing
- Fig.13 Equivalent stress and strain redistributions in a creep-fatigue specimen
- Fig.14 Relationship between the estimated N_f and holding time
- Fig.15 Comparison of the estimated creep-fatigue life results and available test data
- Fig.16 Estimated elastic follow-up factor for plastic behavior (q_p) in a creep-fatigue specimen
- Fig.17 Estimated elastic follow-up factor for creep behavior (q_c) in a creep-fatigue specimen
- Fig.18 Comparison of strain concentration factors for the BM, HAZ, and WM estimated using FEA with those calculated using the rule in the JSME FRs code
- Fig.19 Comparison of the creep damage for the BM, HAZ, and WM estimated using FEA with those calculated according to the rule in the JSME FRs code

Fig.1

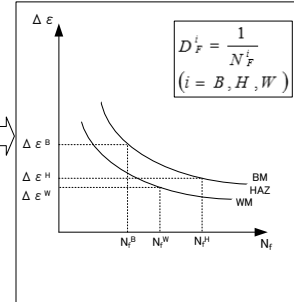
Creep-fatigue test simulation with the entire specimen model



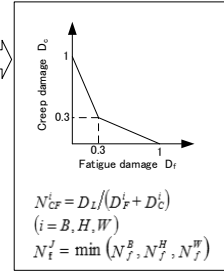
Stress-strain behavior in each region



Fatigue damage evaluation



Creep-fatigue life evaluation



Creep damage evaluation

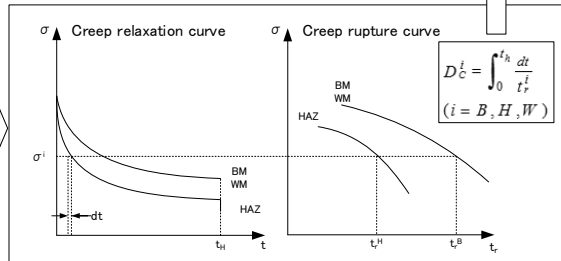


Fig.2

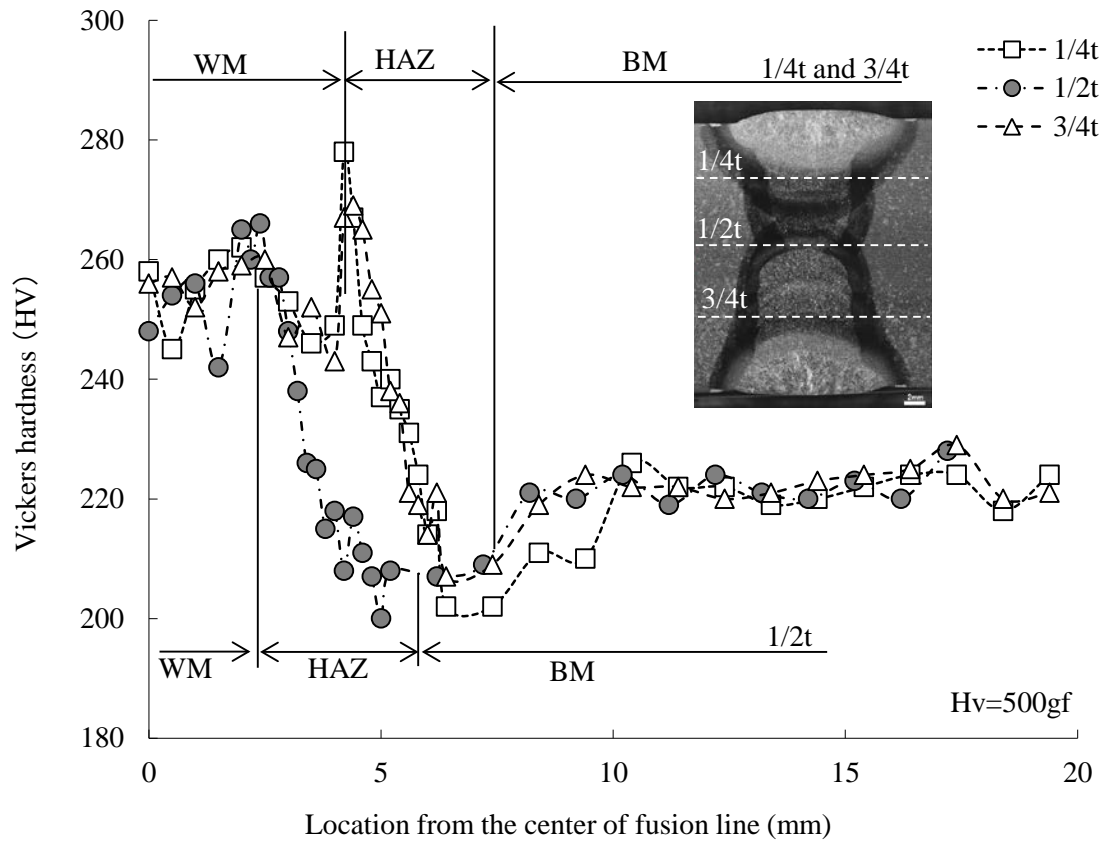


Fig.3

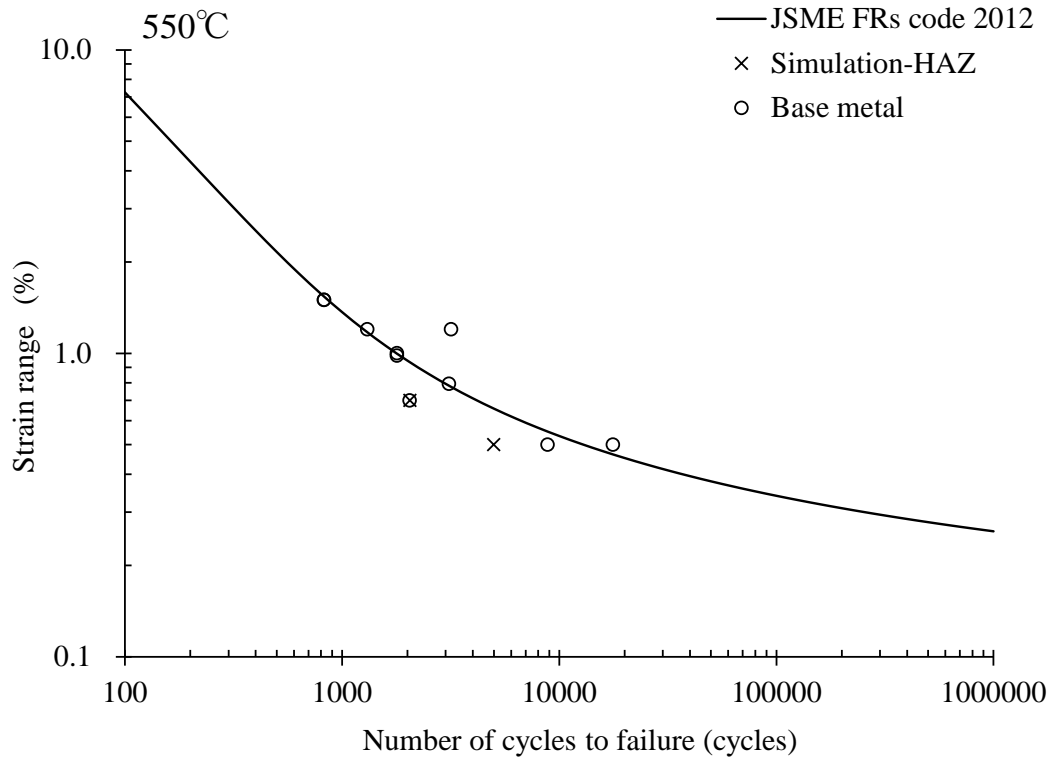


Fig.4

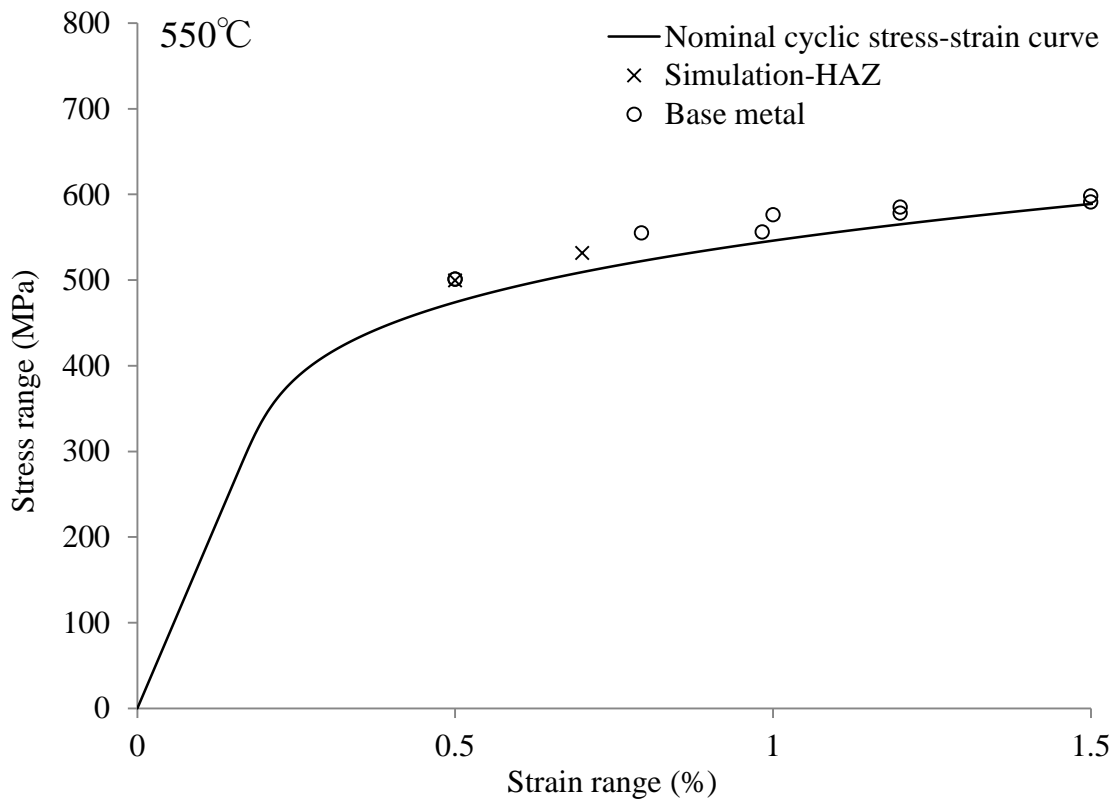


Fig.5

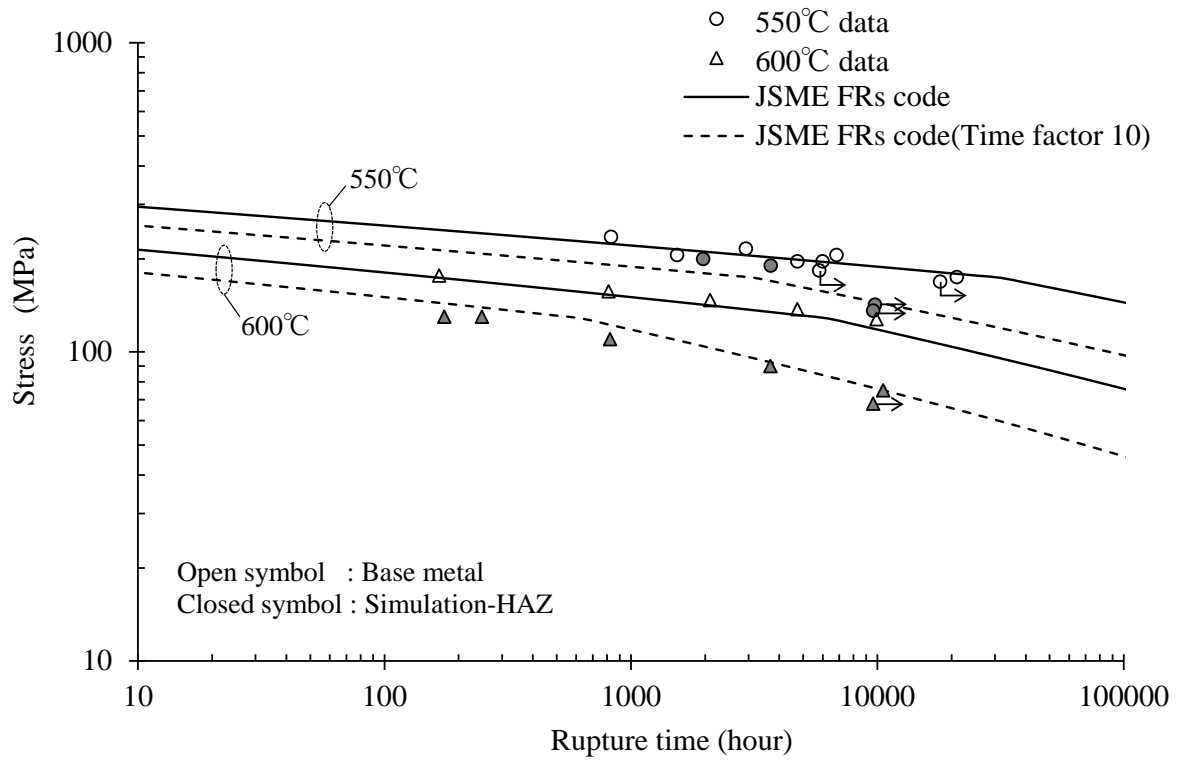


Fig.6

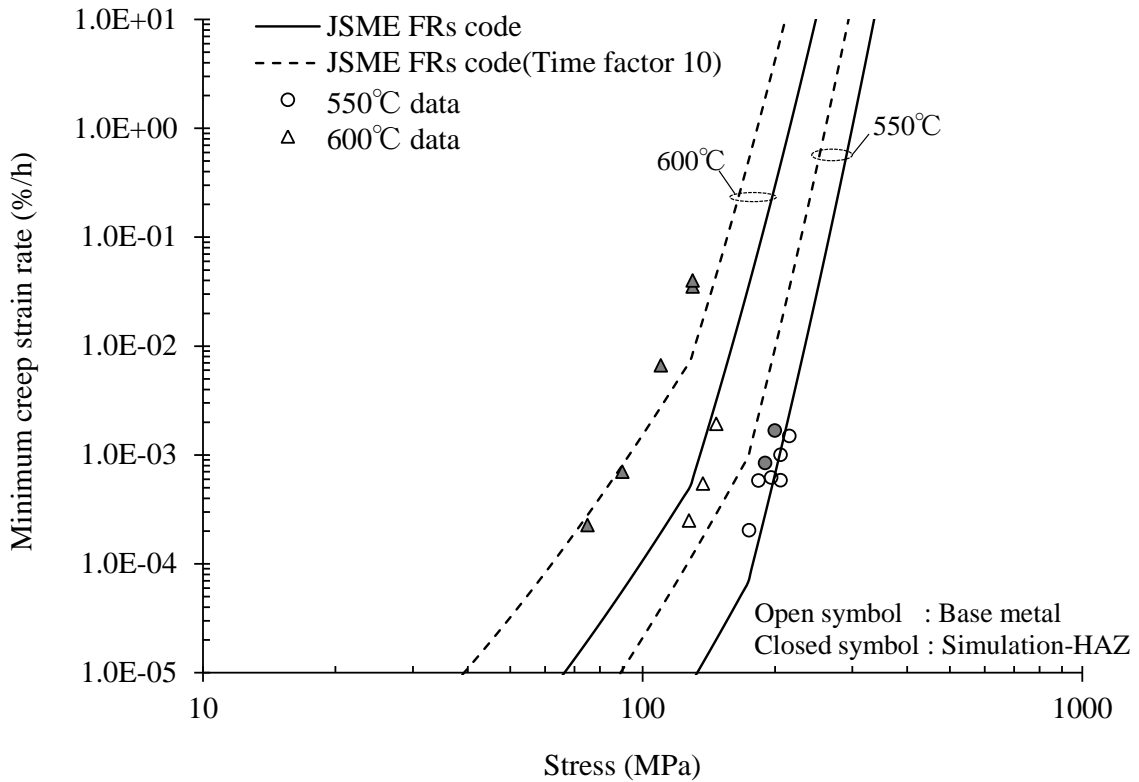


Fig.7

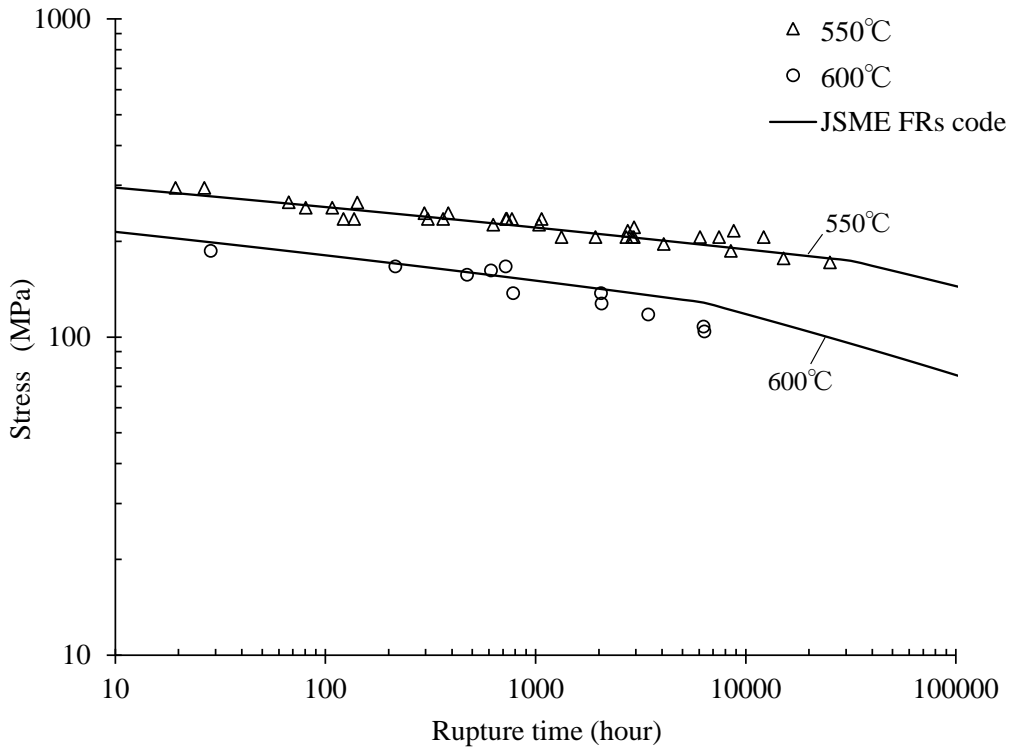


Fig.8

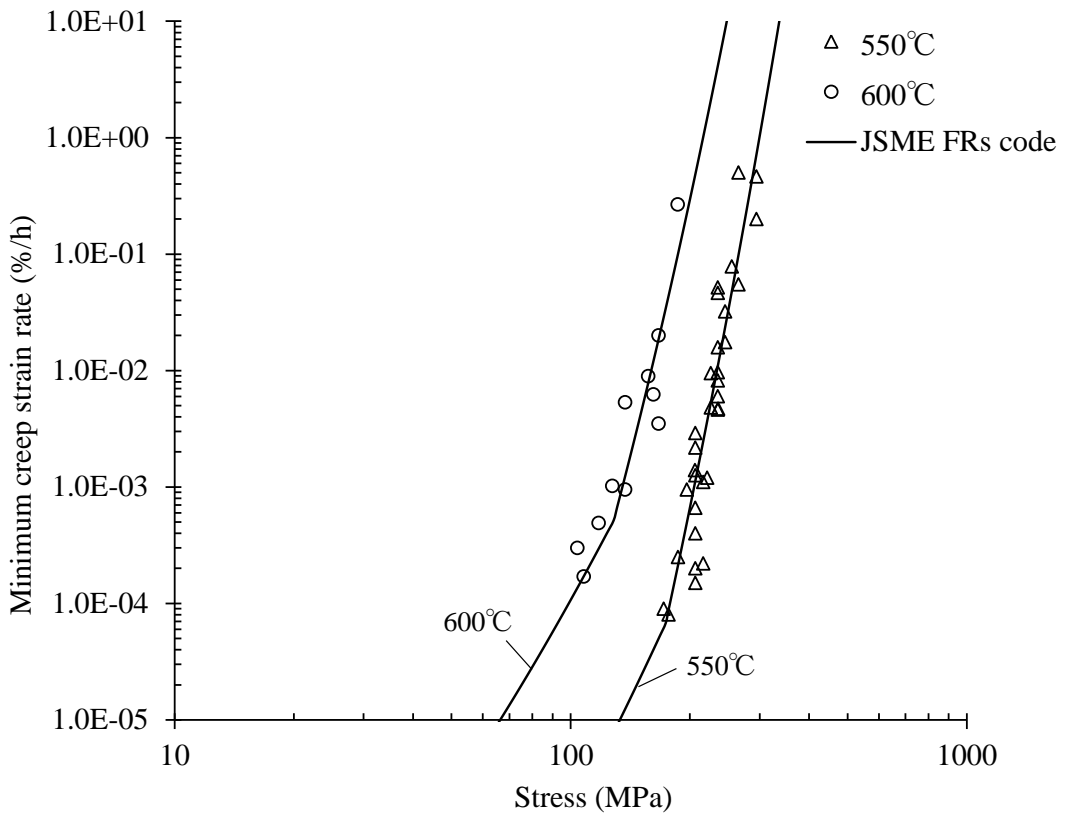


Fig.9

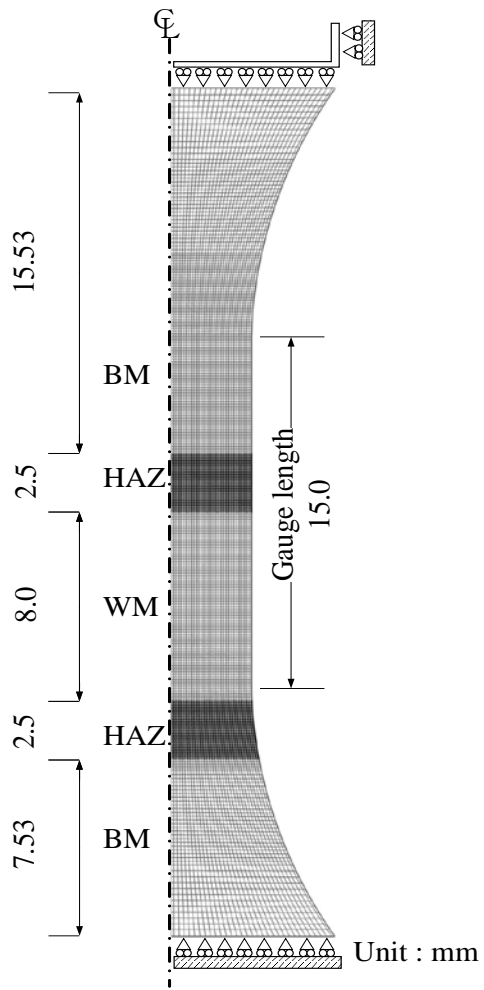


Fig.10

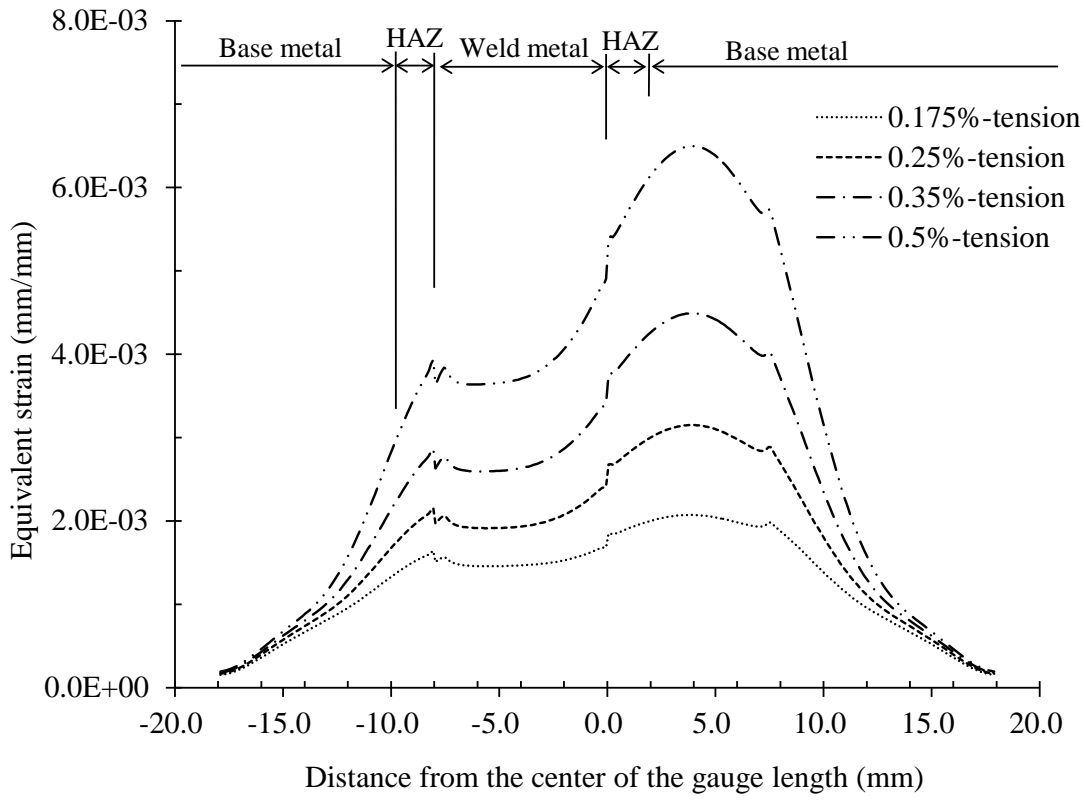


Fig.11

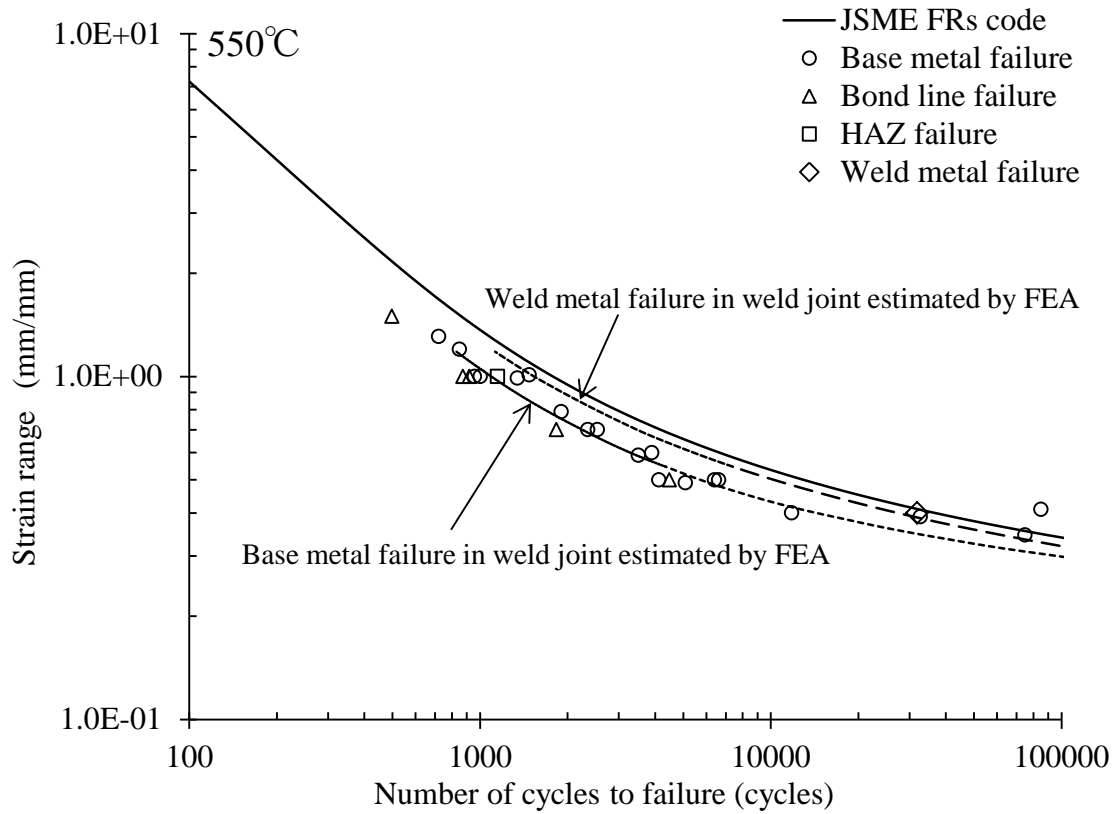


Fig.12

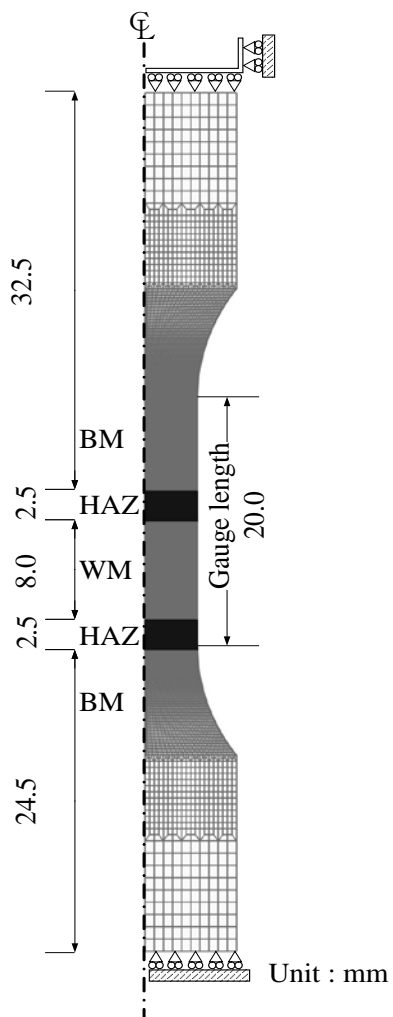


Fig.13(a)

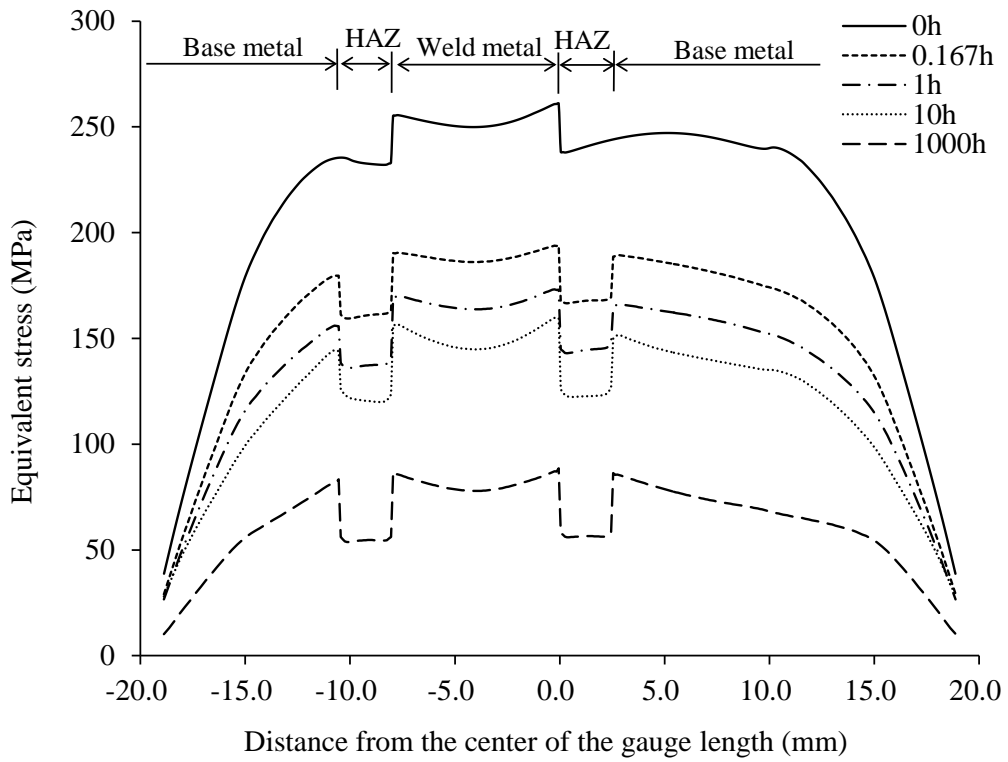


Fig.13(b)

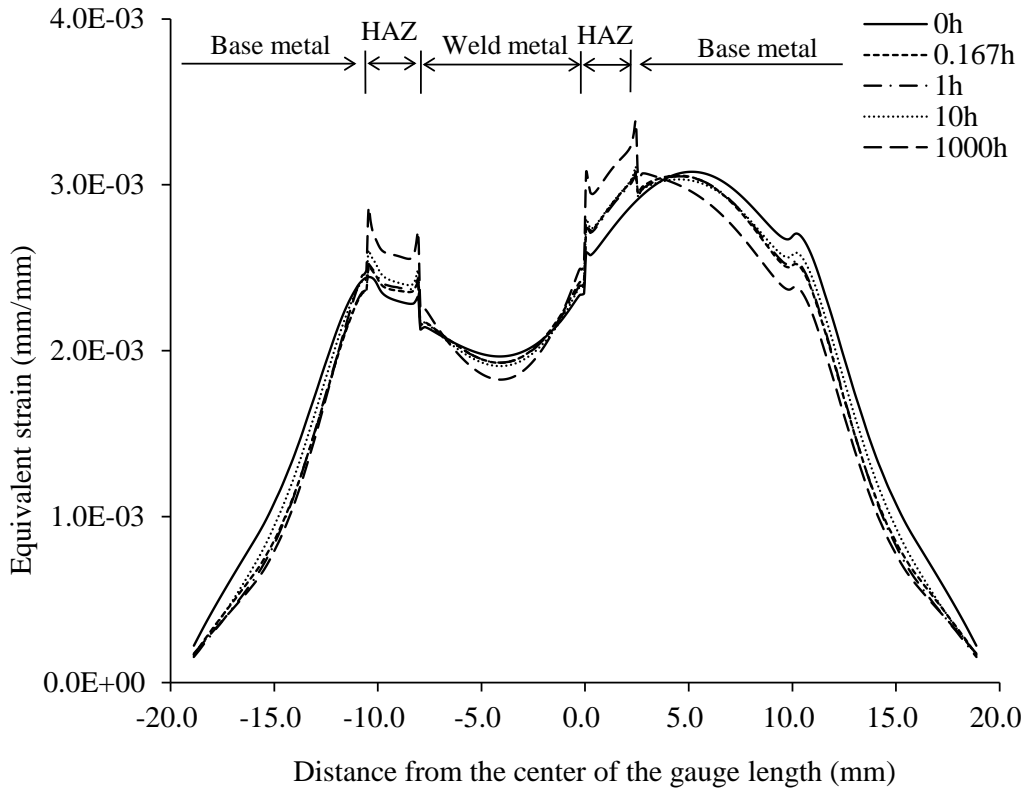


Fig.14(a)

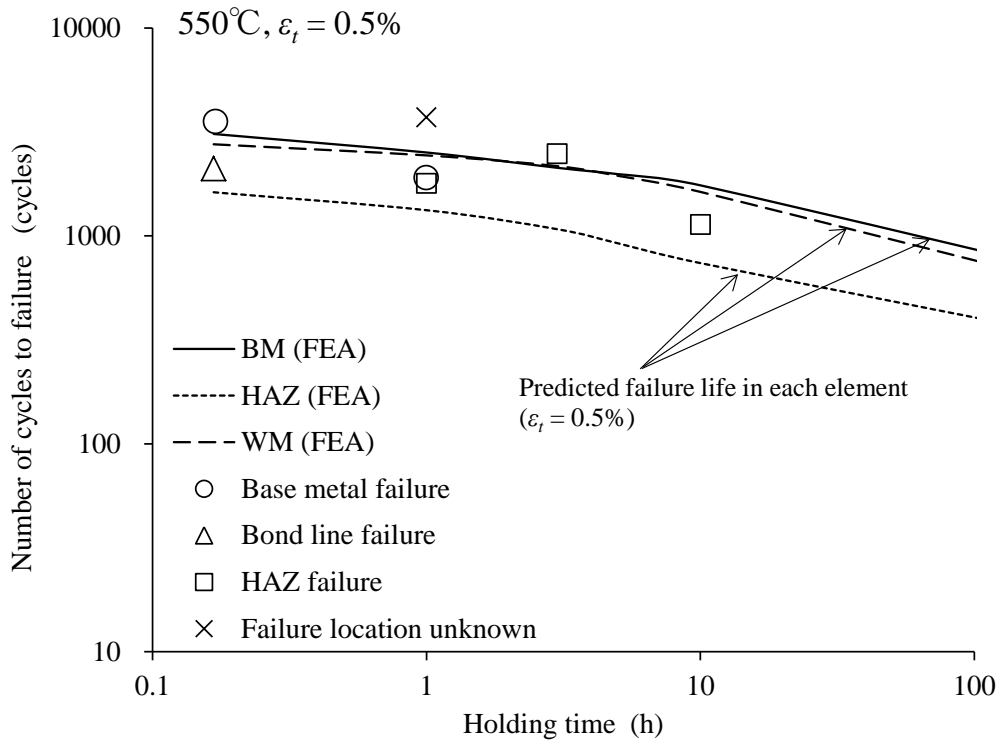


Fig.14(b)

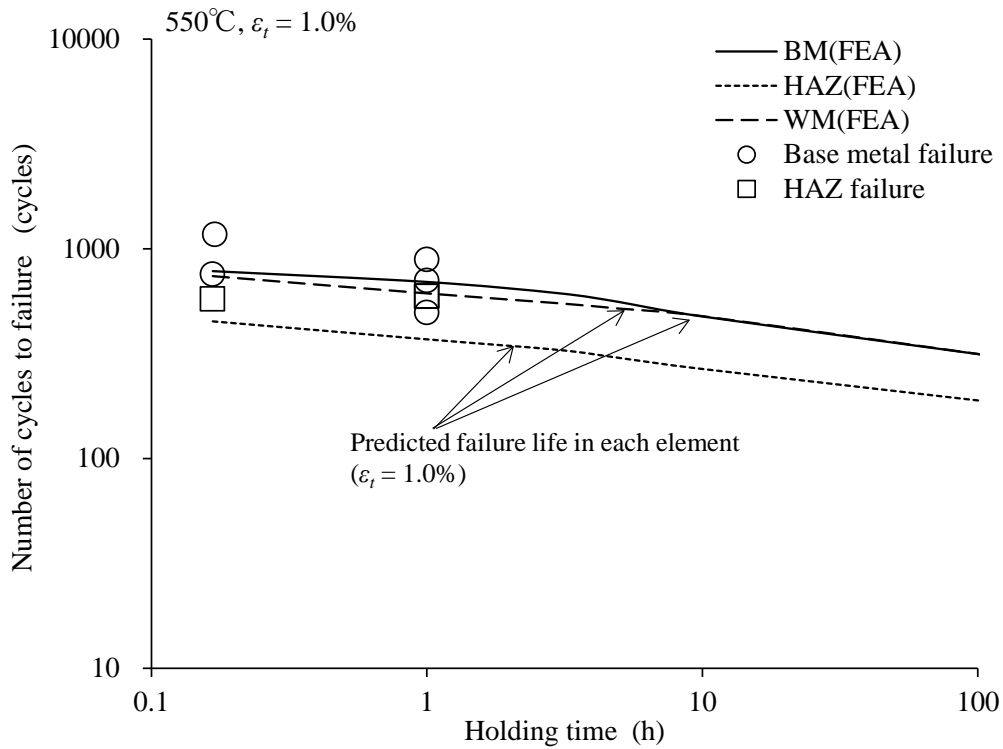


Fig.15

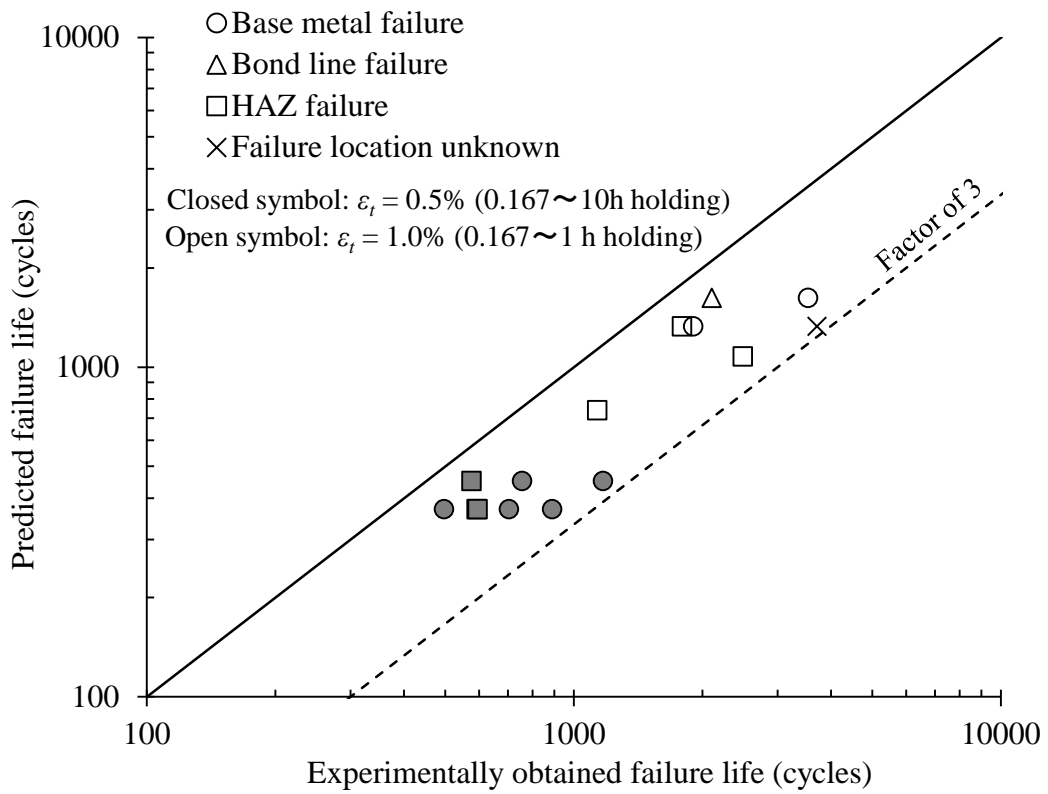


Fig.16

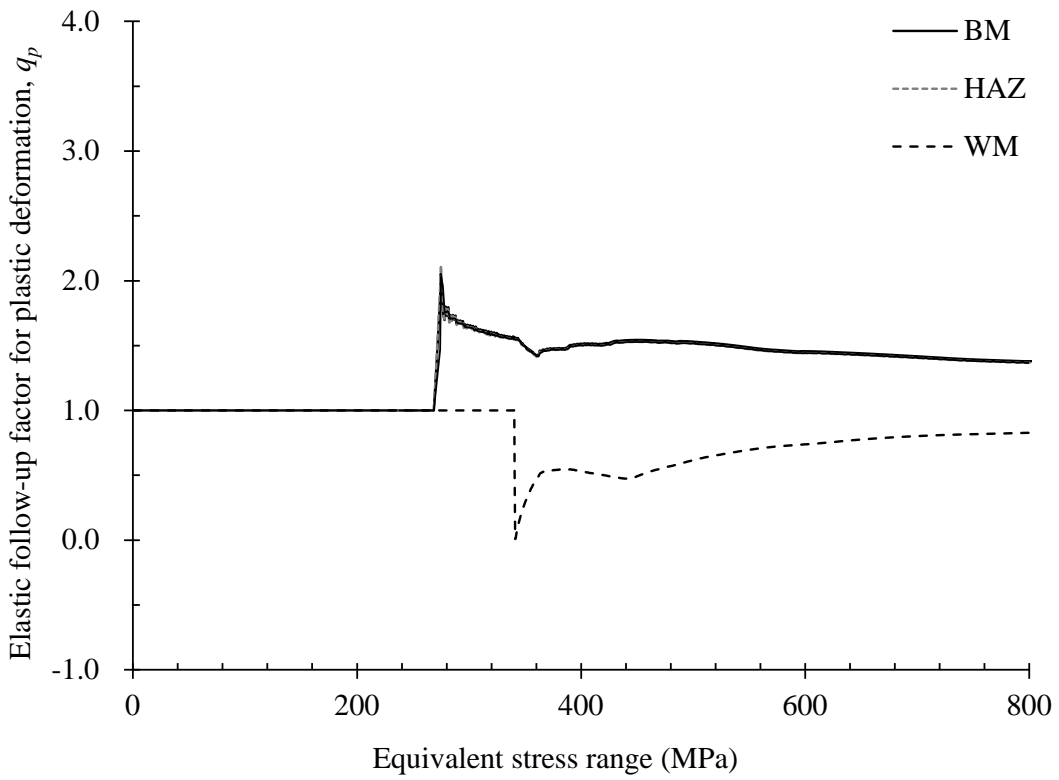


Fig.17

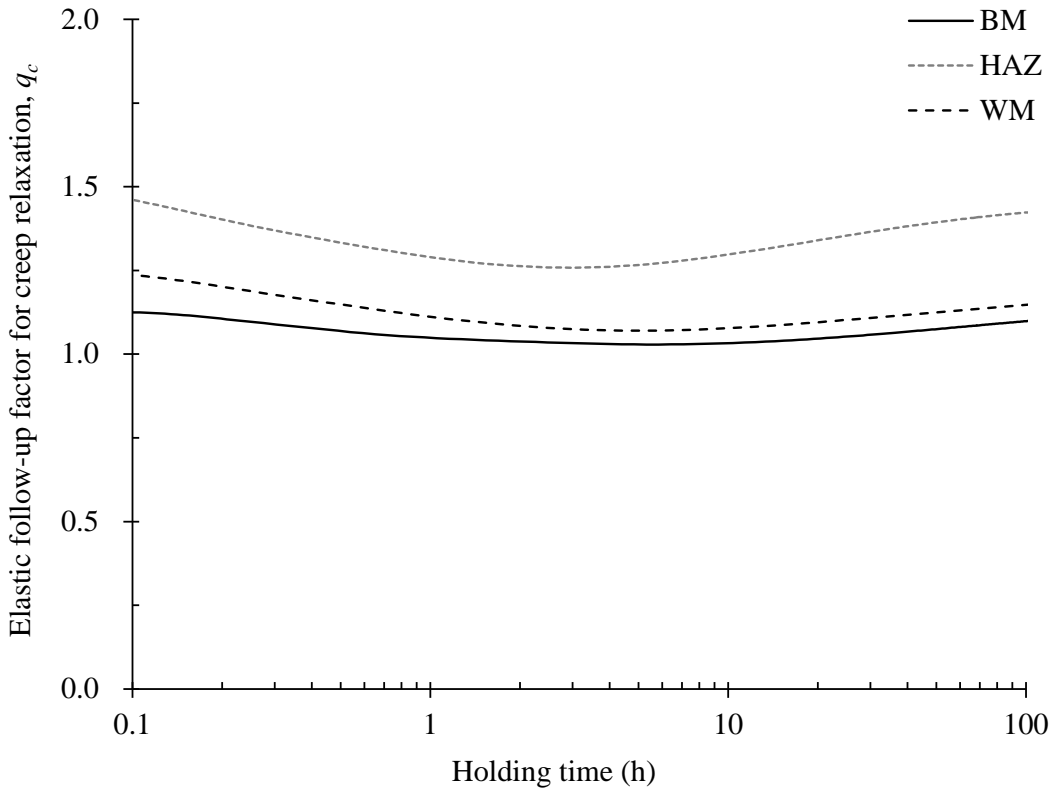


Fig.18

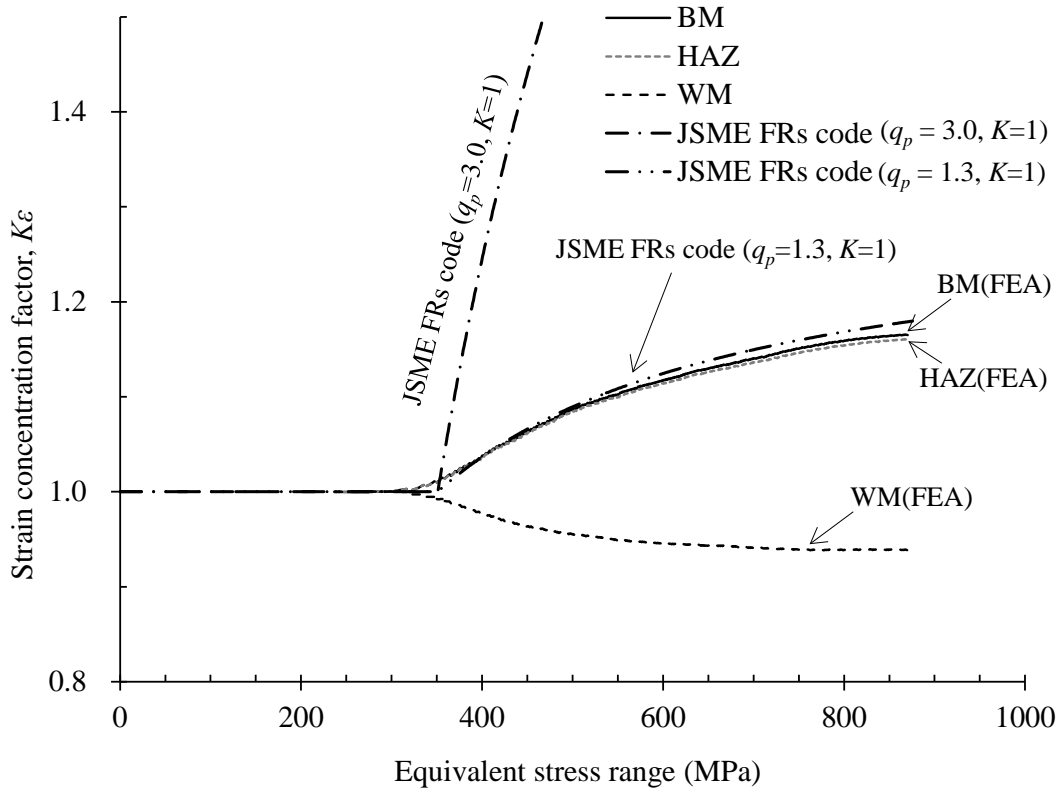
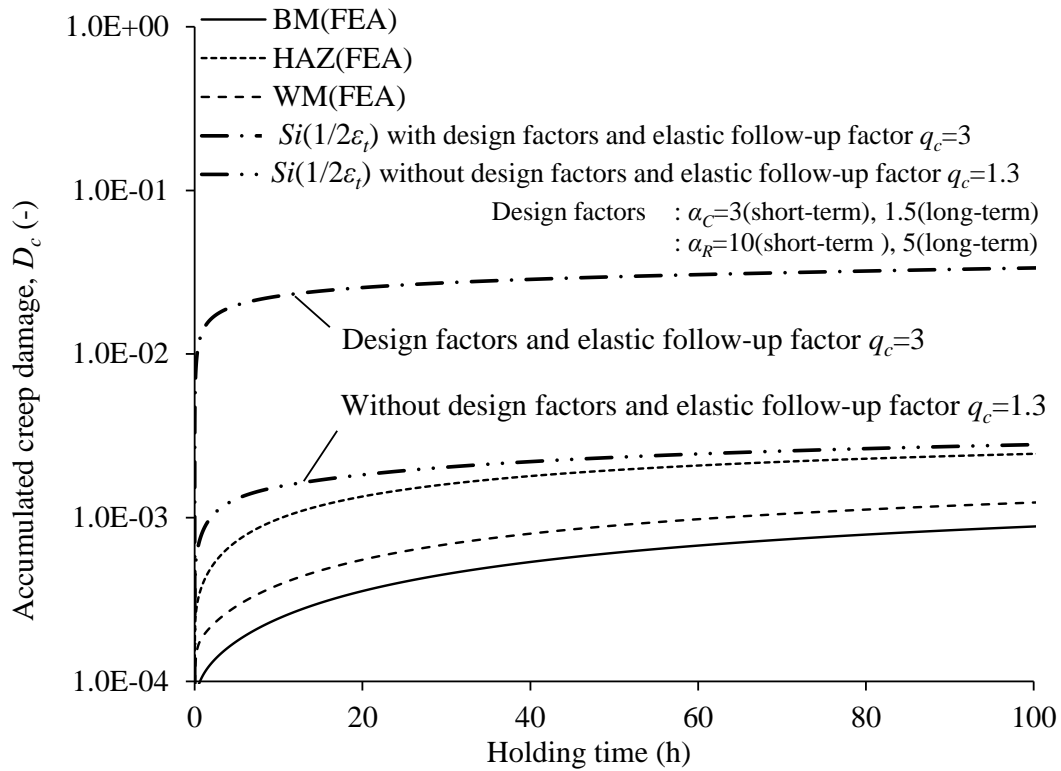


Fig.19



Tables

Table 1 Chemical composition and heat treatment condition of the weld joint

Table 2 Material properties assumed for the three materials used in the FEA

Table A1 Cyclic stress-strain equation of Mod.9Cr-1Mo steel [3]

Table A2 Fatigue life equation of Mod.9Cr-1Mo steel [2]

Table A3 Creep life equation of Mod.9Cr-1Mo steel [2]

Table A4 Creep strain equation of Mod.9Cr-1Mo steel [2]

Table 1

	C	Si	Mn	P	S	Ni	Cr	Mo	Nb	V	N	Cu
Base metal	0.10	0.35	0.43	0.012	0.001	0.05	8.53	0.98	0.08	0.20	0.048	-
Weld metal	0.08	0.16	0.99	0.008	0.007	0.70	8.94	0.89	0.04	0.17	-	0.12

Heat treatment for the BM: 1050 °C for 30 min + 780 °C for 30 min

Post welding heat treatment: 740 °C for 8.4 h

Table 2

Item	BM	HAZ	WM
Elastic modulus	174,000MPa[2]	= BM	= BM
Poisson's rate	0.306[2]	= BM	= BM
Half of cyclic stress-strain response	Table A1[3]	= BM	$1.1 \times \sigma_y$ in Table A1
Fatigue life	Table A2[2]	= BM	$1.1 \times \varepsilon_t$ in Table A1
Creep life	Table A3[2]	$\alpha_R = 10$ in Table A3	= BM
Creep strain rate	Table A4[2]	$\alpha_R = 10$ in Table A3	= BM

Table A1

<p>(1) $\Delta\sigma/2 > \sigma_p$ $\varepsilon_t = \Delta\sigma/E + \{(\Delta\sigma - 2\sigma_p)/K_d\}^{1/m_d}$</p> <p>(2) $\Delta\sigma/2 \leq \sigma_p$ $\Delta\sigma = E \cdot \varepsilon_t$</p> <p><Unit> T : Temperature (°C) $375 \leq T \leq 650$ $\Delta\sigma$: Stress range (MPa) ε_t : Total strain range (mm/mm) E : Elastic modulus (MPa) σ_p : Proportional limit (MPa)</p>	
E	174,000
σ_p	$\sigma_y - K(0.002)^m$
σ_y	$4.94459 \times 10^2 - 4.59540 \times 10^{-1}T + 1.73944 \times 10^{-3}T^2 - 2.68107 \times 10^{-6}T^3$
K	$1.26165 \times 10^3 - 1.69234T$
m	$0.266556 - 3.14984 \times 10^{-4}T$
K_d	$2.71144 \times 10^3 - 2.95792T$
m_d	$2.16634 \times 10^{-1} + 1.09703 \times 10^{-4}T$

Table A2

$(\log_{10} N_f)^{-\frac{1}{2}} = A_0 + A_1 \cdot \log_{10} \Delta \varepsilon_t + A_2 \cdot (\log_{10} \Delta \varepsilon_t)^2 + A_3 \cdot (\log_{10} \Delta \varepsilon_t)^4$	
<Unit>	
T	: Temperature(°C) $RT \leq T \leq 650$ $RT \leq T < 375$: The value of 375 is used
$\&$: Strain rate (mm/mm/s)
ε_t	: Total strain range (mm/mm)
N_f	: The number of cycles to failure
A_0	$1.182614 - 8.971940 \times 10^{-10} \times T^2 \times R^3$
A_1	$6.379346 \times 10^{-1} - 3.220658 \times 10^{-3} \times R$
A_2	$2.065574 \times 10^{-1} + 3.103560 \times 10^{-11} \times T^3$
A_3	-1.168810×10^{-2}
$R = \log_{10} \&$	

Table A3

Creep rupture time is lower value of (1) and (2)	
(1) Short term region	
$\log_{10}(\alpha_R t_R) = -35.25765 + \frac{29368.90}{T + 273.15} + \frac{14217.17}{T + 273.15} \log_{10} \sigma - \frac{5678.093}{T + 273.15} (\log_{10} \sigma)^2$	
(2) Long term region	
$\log_{10}(\alpha_R t_R) = -21.12846 + \frac{26081.50}{T + 273.15} + \frac{818.7218}{T + 273.15} \log_{10} \sigma - \frac{1359.116}{T + 273.15} (\log_{10} \sigma)^2$	
<Unit>	
T	: Temperature(°C) $RT \leq T \leq 650$
σ	: Stress (MPa) $2 \leq \sigma$
t_R	: Creep rupture time(h)
α_R	: Time factor

Table A4

$\varepsilon_c = C_1(1 - e^{-r_1 t}) + C_2(1 - e^{-r_2 t}) + \dot{\varepsilon}_m t$	
<Unit>	
T	: Temperature(°C) $RT \leq T \leq 650$
σ	: Stress (MPa) $2 \leq \sigma$
t_R	: Creep rupture time (h)
$\dot{\varepsilon}_m$: Steady state creep rate (mm/mm/h)
t	: Time (h)
t_R	Table A3
$\dot{\varepsilon}_m$	$2.0416 \cdot \exp\left[-\frac{20197}{8.3144(T + 273.15)}\right] t_R^{-1.1548}$
C_1	$2.1382 \cdot \dot{\varepsilon}_m^{0.59235} / r_1$
C_2	$0.92768 \cdot \dot{\varepsilon}_m^{0.81657} / r_2$
r_1	$317.09 \cdot t_R^{-0.56858}$
r_2	$14.325 \cdot t_R^{-0.82278}$